Chemistry & Biology, Vol. 12, 1211–1219, November, 2005, ©2005 Elsevier Ltd All rights reserved. DOI 10.1016/j.chembiol.2005.08.015

Inspecting the Structure-Activity Relationship of Protein Kinase CK2 Inhibitors Derived from Tetrabromo-Benzimidazole

Roberto Battistutta,[1,3,*] Marco Mazzorana,[2,3] Stefania Sarno,[2,3] Zygmunt Kazimierczuk,[4] Giuseppe Zanotti,[1,3] and Lorenzo A. Pinna[2,3,*]

[1]Department of Chemistry
University of Padua
via Marzolo 1
35131 Padua
Italy

[2]Department of Biological Chemistry
University of Padua
viale G. Colombo 3
35121 Padua
Italy

[3]Venetian Institute for Molecular Medicine–VIMM
Padua
Italy

[4]Laboratory of Experimental Pharmacology
Polish Academy of Sciences Medical Research Center
Warsaw
Poland

Summary

CK2 is a very pleiotropic protein kinase whose high constitutive activity is suspected to cooperate to neoplasia. Here, the crystal structure of the complexes between CK2 and three selective tetrabromo-benzimidazole derivatives inhibiting CK2 with K_i values between 40 and 400 nM are presented. The ligands bind to the CK2 active site in a different way with respect to the parent compound TBB. They enter more deeply into the cavity, establishing halogen bonds with the backbone of Glu114 and Val116 in the hinge region. A detailed analysis of the interactions highlights a major role of the hydrophobic effect in establishing the rank of potency within this class of inhibitors and shows that polar interactions are responsible for the different orientation of the molecules in the active site.

Introduction

Protein kinases, which catalyze the transfer of the γ phosphate of ATP (and, seldom, GTP as well) to serine, threonine, and tyrosine residues of protein substrates, play a central role in controlling nearly all cellular functions, with special reference to signal transduction. They make up one of the largest families of enzymes, with more than 500 members encoded by the human genome [1] and often unscheduled and/or constitutive activation of individual protein kinases underlies pathologies [2]. Consequently, the development of efficient and selective inhibitors of protein kinases represents a powerful tool for unraveling the functional implication of individual kinases and, in some cases, it may also provide leads with pharmacological potential. Indeed, protein kinases now represent the second most important target for therapeutic agents [3, 4]. Several protein kinase inhibitors are already in advanced clinical trials, or even in clinical practice, to cure tumors and other diseases [3, 5, 6]. Interestingly, most of these inhibitors are competitive with respect to ATP, a circumstance that could sound surprising, given that the ATP binding site is highly conserved in all members of the protein kinase family. The explanation for such an apparent incongruence was provided by the solution of the crystal structure of complexes between protein kinases and a number of ATP site-directed inhibitors (reviewed in [7]), revealing that these do not exactly mimic the mode of binding of ATP but rather occupy a region adjacent to and partially overlapping the actual ATP binding site. This region, mainly composed of the hinge segment connecting the upper and lower lobes of the kinase and two hydrophobic pockets, displays sufficient variability across protein kinases to be exploited to harbor specific ligands [8]. In this respect, the solution of the crystal structure of complexes between kinases and ATP site-directed ligands represents the most powerful tool for scrutinizing the mode and structural consequences of binding of these compounds and for the design of more potent and selective inhibitors ([7, 9–11] and references therein).

Specific inhibitors are especially needed in the case of constitutively active protein kinases, which, unlike most other members of the family, are not activated in response to specific stimuli—nor do they exist within the cell as inactive and active forms, generally distinguishable for different degrees of phosphorylation. Therefore, alternative tools such as physiological agonists/antagonists, phosphospecific antibodies, and transfection with constitutively active mutants (where the phosphoresidue responsible for activation has been mimicked by a carboxylic side chain) are not applicable to dissecting the cellular functions mediated by constitutively active kinases. Highly selective, cell-permeable inhibitors remain among the few applicable strategies for gaining information about the biological roles of constitutively active protein kinases.

A striking example of constitutively active protein kinase is provided by CK2, an acronym derived from the misnomer "casein kinase-2." CK2 is the most pleiotropic Ser/Thr kinase known to date, with a growing list of more than 300 protein substrates, many of which are implicated in a variety of important cellular functions, with special reference to signal transduction, gene expression, and DNA synthesis and repair [12]. CK2 catalytic subunits (α and α') are constitutively active either alone or in combination with the regulatory β subunit to give a heterotetrameric holoenzyme composed by two catalytic subunits held together by a β_2 dimer, functioning as a docking and/or targeting element rather than as a canonical regulatory subunit [13–16]. It has been suggested that constitutive activity of CK2 may reflect its extraordinary pleiotropy, which would be hardly compatible with the necessity of keeping quiescent CK2 activity within a living cell at any moment [13]. On the other hand, such a lack of downregulatory mechanisms may

*Correspondence: roberto.battistutta@unipd.it (R.B.), pinna@civ.bio.unipd.it (L.A.P.)

also underlie the pathogenic potential of CK2, disclosed by an increasing number of observations. CK2 activity is invariably elevated in many different kinds of tumors (reviewed in [17]), and overexpression of its catalytic subunits is causative of neoplastic growth in animal and cellular models presenting alterations in the expression of cellular oncogenes or tumor suppressor genes [18–21]. Also remarkable in this context is the increasing evidence that CK2 plays a global antiapoptotic role [22], which could account for its implication in those kinds of tumors, exemplified by prostate carcinoma, whose key feature is deregulation of programmed cell death. An added value of CK2 inhibitors could also be their exploitation in infectious diseases, in that many viruses depend on host cell CK2 for the phosphorylation of proteins that are essential to their life cycle [17].

Not surprisingly, therefore, an increasing number of recent reports deal with pharmacological inhibition of CK2 by a variety of compounds. These include flavonoids, notably apigenin [23] (whose selectivity, however, is quite modest [24]), emodin [25], and other condensed polyphenolic compounds [26], the indoloquinazolin derivative IQA [24, 27], and a variety of halogenated benzimidazole/triazole compounds developed from the original molecule DRB [28, 29]. The one most successfully used at present is 4,5,6,7-tetrabromo-1-benzotriazole (TBB), a very selective, cell-permeable CK2 inhibitor [30] that is proving useful in documenting the implication of CK2 in a variety of cell functions (notably apoptosis [31], repair of chromosomal DNA single-strand breaks [32], functionality of the pleiotropic cochaperone CDC-37 [33], and upregulation of the Akt signaling pathway [34]) and in identifying new protein targets of CK2 (reviewed in [35]). Recently, the inhibitory properties of TBB have been further improved by the generation of a number of tetrabromo-benzimidazole derivatives, some of which display the same selectivity and cell permeability of the parent compound but a higher inhibitory efficacy, with K_i values in the low nanomolar range [36]. Here we describe the crystal structure of three of these compounds, bound to the active site of the catalytic subunit of CK2. The data collected, in conjunction with those of the TBB complex and of the apoenzyme [37], allow a detailed structure-activity relationship study of this class of CK2 inhibitors and provide valuable hints for the design of more selective and potent inhibitors.

Results and Discussion

TBB is a cell-permeable, selective, and fairly potent CK2 inhibitor that has been successfully used to validate the involvement of this pleiotropic kinase in different cellular events (see Introduction). The shape and the reduced dimension of the CK2 ATP binding site were proposed to play a key role for determining the selectivity of this inhibitor [37]. Accordingly, mutagenesis studies have highlighted the relevance of the unique residues Ile/Val66 and Ile174, whose replacement by alanine decreases susceptibility of CK2 to TBB inhibition. Recall in this respect that the hydrophobic moiety of protein kinase ATP binding sites is more variable than the polar one, which is highly conserved. Selectivity therefore is better ensured by interactions with the hydrophobic region [38, 39].

Several TBB derivatives have been recently synthesized and tested on CK2 in the attempt to improve the inhibitory properties [36]. For those with the lowest inhibitory constants, crystallization trials have been set up in complex with the *Zea mays* CK2 α-catalytic subunit, whose active core is nearly identical to that of its human homolog. Three of these, namely K25 (also termed DMAT; see [40]), K44 (whose synthesis is described here), and K37 [36], have produced crystals diffracting to a reasonable resolution (see Table S1 for data collection statistics). Note that K25 displays a K_i value for CK2 of 40 nM, the lowest reported in the literature for a CK2 inhibitor. Its selectivity and cell permeability are similar to those of TBB, rendering K25/DMAT the first choice CK2 inhibitor for in-cell studies.

Synthesis of K44 (N^1,N^2-Ethylene-2-Methylamino-4,5,6,7-Tetrabromo-Benzimidazole)

Compound **2** (Scheme S1) was obtained by amination of 2,4,5,6,7-pentabromobenzimidazole **1** [41] with 2-(methylamino)ethanol. The reaction of the hydroxyalkyl compound **2** with thionyl chloride gave a chloroalkyl derivative, which was cyclized to compound **3** upon heating in ethanolic solution in the presence of DBU (1,8-diazabicyclo[5,4,0]undec-7-ene) as base. Attempts to isolate the chloroalkyl intermediate were unsuccessful, due to partial cyclization during crystallization. The detailed synthesis procedures are described under Experimental Procedures. The chemical structures of newly obtained products were confirmed by elemental analyses, ^{1}H NMR, and mass spectroscopy.

Structural Effects on CK2 upon TBB-Derivatives Binding

Like TBB, the three new derivatives are ATP-competitive and, as expected, they occupy the ATP binding region between the N-terminal and the C-terminal lobes of the enzyme. The overall three-dimensional structure of the enzyme is essentially conserved, with only minor changes in some flexible residues facing the binding pocket. The major variations are seen in the conformation of the Gly-rich loop and of the hinge region, as well as in the side chains of His160 and Met163. In the K44 complex, a rearrangement in the electrostatic interactions between the charged Lys68, Glu81, and Asp175 is observed (as discussed in detail below). As seen for other CK2 complexes [6, 11, 24, 37, 42, 43], the flexible loop 102–108 adopts an extended conformation that corresponds to a "longer" b unit cell axis of around 59-61 Å and a β angle of approximately 103–104° (instead of values of approximately 52 Å and 99°, respectively, corresponding to the loop in a bent conformation; see also Experimental Procedures).

In the CK2 complexes with Emodin and TBB, the His160 side chain was displaced from its original position, thus entrapping the ligand inside the binding pocket. The flexibility of this side chain is confirmed by the fact that in the CK2/K44 complex it is clearly visible in a double conformation, one pointing to the solvent and the other to the binding site; this latter conformation is similar to that of the Emodin complex.

Apart from Emodin, in all other CK2-inhibitor complexes a conserved water molecule was always found hydrogen bonded to the Trp176 backbone nitrogen

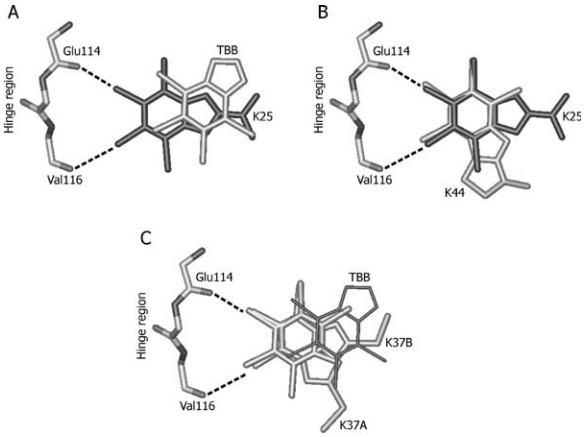

Figure 1. Superpositions of K25

Superpositions of K25 with TBB (A) and with K44 (B); the two conformations A and B of K37 are also shown (C). The TBB position is indicated as reference. The interactions with Glu114 and Val116 of the hinge region of CK2 (halogen bonds) are indicated by dashed lines. Note the similar orientation of K37A with K44 and of K37B with K25.

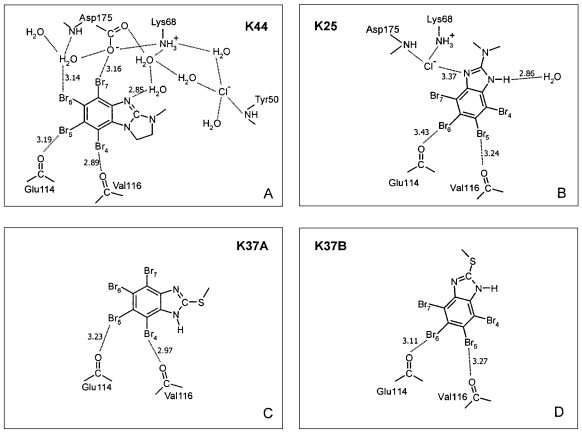

Figure 2. Polar Interactions

Polar interactions between CK2 and K44 (A), K25 (B), and K37 in conformation A (C) and conformation B (D). Only distances (in Å) between the inhibitors and the protein atoms are indicated. Note the different location of the chlorine ions in panel A (Cl^- far from the inhibitor K44) and B (Cl^- ion paired with Lys68 can directly interact with K25). The parent compound TBB (not shown) does not make any direct polar interaction with CK2 residues of the active site.

and Glu81 side chain carboxyl function [11]. This water molecule is also present in all three of the new structures here described.

Polar Interactions between CK2 and Inhibitors

In the binding cavity, K25, K44, and K37 lie essentially in the same plane of TBB but penetrate deeper, reaching the hinge region. Each derivative makes two direct interactions with the same elements of this region (i.e., the backbone carbonyls of Glu114 and Val116) (Figure 1); these residues are pushed back with respect to their position in the TBB bound complex and in the apoenzyme. Note that these are the same residues that interact with the adenine moiety of ATP when bound to the active site [44]. In all cases, the inhibitors interact with the hinge region through two bromine atoms, at a distance between 2.9 and 3.4 Å from the carbonyl oxygen atoms. The nature of this interaction has been already discussed in the case of CDK2 protein kinase in complex with TBB [45]. It consists of a weak noncovalent interaction shown to occur between carbon-bonded halogens (Cl, Br, or I) and electronegative atoms (notably O and N), called a halogen bond, with a strong directional preference, mainly due to electrostatic effects that arise from an anisotropic electronic distribution of the halogen atoms [46, 47]. In our complexes, the distances between the bromine and the oxygen atoms (between 2.9 and 3.4 Å, less than or equal to the sum of the van der Waals radii of oxygen, 1.52 Å, and bromine, 1.85 Å) and the directionality of the interactions (angle C—Br ····· O close to the optimal value of 165°) are consistent with an attractive interaction. In general, the stabilizing effect of a halogen bond is estimated between about half to slightly more than that of hydrogen bonds, depending on the geometry of the interaction. For K44, two additional halogen bonds are established by Br6 and Br7, with a water molecule and the Asp175 side chain, respectively (see Figure 2A), totaling four halogen bonds, one for each bromine atom.

As in the case of the TBB parent molecule, there are no direct hydrogen bonds between any of the TBB-derivatives atoms and the protein, and only a few with water molecules, as illustrated in Figure 2. A further polar interaction is established by a nitrogen atom of K25 that is at a van der Waals distance to a chlorine ion (Figure 2B), in such a way that a polar electrostatic interaction can be hypothesized between the two. A chlorine ion is evident also in the K44 structure, where however it does not interact with the inhibitor.

Overall, taking into account only the polar interactions just described, it is difficult to explain the differences in the experimental values of IC_{50} and K_i. For instance, although K44 is the inhibitor with the highest number of polar interactions with the protein, nevertheless it has an inhibitory potency lower than that of K25, which makes fewer polar contacts with CK2. Furthermore, looking at only these interactions it is not clear why TBB is a better inhibitor for CK2 than for the protein kinase CDK2, with which it is able to form four halogen bonds [45].

Apolar Interactions between CK2 and Inhibitors

In the attempt to correlate the contribution of the apolar interactions (i.e., van der Waals interactions and hydrophobic effect) to the binding of different inhibitors, two types of analysis were performed, based on (1) the number of van der Waals contacts between CK2 and the inhibitors (with two cutoffs of 3.7 and 3.9 Å) and (2) the amounts of the accessible surface area buried (ΔASA) upon binding of the inhibitors to CK2. Details about both analyses performed are described in the Experimental Procedures section and the main results are shown in Table 1, together with the IC_{50} and K_i values. As in the case of the polar interactions, the number of the van der Waals contacts seems not to correlate with the inhibitory potency (Table 1). For instance, K25 makes the lowest number of contacts even though it presents the lowest K_i. In contrast, a reasonable correspondence is observed between the inhibitory potencies and the

Table 1. Number of van der Waals Contacts (vdW) between Inhibitors and Proteins and Accessible Surface Areas Differences (ΔASA in Å^2) upon Ligand Binding

	vdW		ΔASA (Å^2)				
	≤3.7 Å	≤3.9 Å	ΔASAin	ΔASAprot	ΔASAtot	IC_{50}	K_i
TBB-CDK2	9	19	342.2	192.9	535.1	15.6	—
TBB-CK2	13	19	375.4	206.0	581.4	0.50	0.40
K44	12	24	379.5	214.6	594.1	0.74	0.10
K37_Aver	15[a]/18[b]	28[a]/31[b]	397.1	231.2	628.3	0.25	0.07
K25	9	22	413.1	259.1	672.2	0.14	0.04

ΔASAin, ΔASA inhibitor; ΔASAprot, ΔASA protein; ΔASAtot: ΔASA total, sum of ΔASA inhibitor and ΔASA protein; K37_Aver: values averaged between the two conformations.
[a] Values relative to conformation A of K37.
[b] Values relative to conformation B of K37.

total accessible surface areas buried upon ligand binding to CK2 (ΔASAtot values in Table 1). Note that these areas are mostly apolar on both sides, supporting the assumption that the extent of the surface areas no longer accessible to the solvent is proportional to the strength of the hydrophobic interaction. This contribution arises from the entropic gain due to the transfer of water molecules from the hydrophobic surfaces of the CK2 binding site and the inhibitors to the bulk solution. From the plot of the logarithmic values of the K_i and IC_{50} versus the ΔASAs, a linear relationship between these parameters could be obtained (see Figure 3).

Although the hydrophobic effect alone can explain the differences in the potencies within this class of inhibitors, a fundamental contribution to the overall energetic of binding must be attributed also to the van der Waals interactions, as demonstrated by the importance of the presence in the inhibitors of bromine atoms instead of other halogens with different van der Waals radii [37].

Relative Influence of the Hydrophobic Effect and Polar Interactions in the Binding of TBB-Derivatives to CK2

The analysis reported in the preceding sections supports the notion that the hydrophobic effect is principally responsible for the differences in the inhibitory potency of TBB and its derivatives against CK2. For instance, despite K44 shows a more extensive network of polar interactions, and it has an inhibitory constant K_i higher than that of K25, in accordance with the lower ΔASA of binding, 594 versus 672 Å [2].

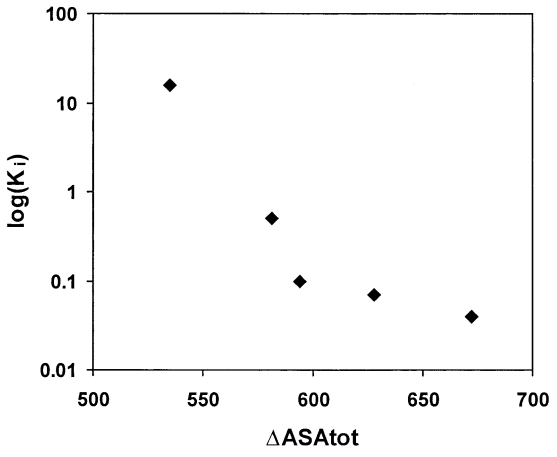

Figure 3. Correlation between Log(K_i) and Values of ΔASAtot for the Different Inhibitors

For TBB-CDK2, the log(IC_{50}) is reported, as in Table 1.

The polar interactions, however, appear to play a role in orienting the ligands inside the active site. Note that, although the positions of the three molecules inside the ATP binding pocket are similar, the respective orientations are quite different, as highlighted by the bromines that interact with Glu114 and Val166: these are Br5 and Br6 in the case of K25, and Br4 and Br5 in the case of K44 (Figures 1, 2A, and 2B). Concerning K37, two orientations have been found in the crystal structure; Br4 and Br5 interact with the hinge region in one case (conformation A), and Br5 and Br6 in the other case (conformation B), with an occupancy of 60% and 40%, respectively (Figures 1, 2C, and 2D). Conformation A of K37 resembles that of K44 (Figures 2A and 2C) and conformation B resembles that of K25 (Figures 2B and 2D). These dissimilar orientations of the inhibitors can be ascribed mainly to small but relevant differences in the dimensions, electronic configurations, and polarizability of these small ligands.

The crystal structures of the K25 and K44 complexes disclose the presence of chlorine ions inside the binding site in a way that causes a rearrangement in the local electrostatic field of the polar moiety of the cavity. In the case of K44, the presence of a chlorine ion contributes to the displacement of two residues conserved among protein kinases and crucial for the activity of the enzyme, Lys68 and Asp175, now at an ion-pair distance (Figure 4). These residues are now part of a complex network of polar interactions, involving the chlorine ion, several water molecules and two bromine atoms (Br6 and Br7) and a nitrogen of the inhibitor (Figure 2A). In the case of K25, a chlorine ion is close to an aromatic nitrogen of K25 and is stabilized by the amine function of the Lys68 side chain and by the amide nitrogen of the Asp175 backbone (Figure 2B).

From a superimposition of the crystal structures, it turns out that TBB binds to protein kinase CDK2 in a way very similar to that of K25 bound to CK2, with the same bromine atoms interacting with corresponding residues of the hinge region (Glu81 and Leu83 for CDK2, Glu114 and Val116 for CK2, respectively). The different modes of interaction of TBB with the active sites of CK2 and CDK2 can be attributed to a variation in the shape and dimension of the two cavities, with special

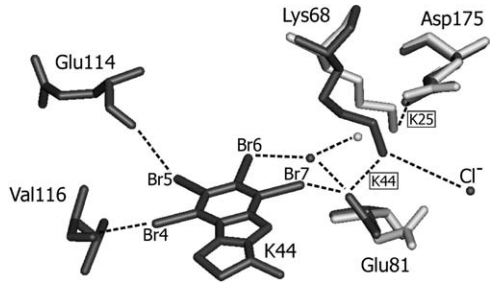

Figure 4. K44 Interactions

Main interactions (dashed lines) of K44 in the active site of CK2 are shown. Note the four halogen bonds between K44 bromine atoms and the protein and the different conformations of Lys68 and Glu81 (dark gray) compared to that in the K25 complex (light gray). This rearrangement is favored by the presence of a negative chlorine ion near the positive amine function of Lys68. The positions of two water molecules part of the network of interactions are indicated by small spheres.

regard to their apolar regions; in both cases, the main contribution to the binding energy is due to the hydrophobic effect. This effect is higher in the case of CK2, as indicated by the different ΔASA: 535 Å^2 for CDK2 and 581 Å^2 for CK2. This may be due, at least partially, to the replacement of two bulky side chains of CK2, those of Ile/Val66 and of Ile174, by alanines in CDK2. Note that the amino acids with higher values of ΔASA upon ligand binding to CK2 are Val45, Val53, Ile66, Met163, Ile174, and Asp175 (Table 2 and Figure 5). Three of these (Ile66, Met163, and Ile174) are unique for CK2 and are those that presumably contribute to a greater extend to the diversity of the ATP binding site, which is smaller than in the majority of the other kinases as indicated by the unusually low sensitivity of CK2 to staurosporine and by its selectivity for TBB and related compounds. The fact that Asp175 also shows a remarkable variation in the value of ΔASA is in accordance with its function in coordination of a Mg^{2+} ion when an ATP molecule is bound.

Like the parent compound TBB, the three derivatives dealt with in the present study inhibit CK2 more potently than CDK2, as shown by their IC_{50} values (Table 3). Note, however, that the ratio between IC_{50} values and the two kinases denotes an improvement of their relative efficacy toward CDK2, especially remarkable in the case of K37. Again, the small size of the CK2 active site compared to that of CDK2 seems to be important in this respect; overall, the decrease in the IC_{50}(CDK2/CK2) ratios can be explained with the increased dimension of the derivatives compared to TBB, suggesting that they can better interact with the larger cavity of CDK2. On the other hand, the trends of the IC_{50} ratios and CDK2 IC_{50} values are difficult to completely rationalize in absence of the corresponding experimental crystal structures.

Although the effect of mutating Met163 could not be assessed because the M163G mutant proved catalytically inactive [35], the importance of Ile66 and Ile174 was experimentally validated by mutational studies by which Val66 (the homolog of Ile66 in human CK2) and Ile174 were individually or collectively mutated to one or more alanines. These mutations were detrimental to the inhibitory potency of a variety of compounds, including TBB and K25 (DMAT), but increased the inhibitory efficiency of staurosporine [26].

Table 2. Residues with the Higher Accessible Surface Areas Differences (ΔASA in Å^2) upon Ligand Binding

ΔASA (CK2)	TBB	K25	K44	K37_A	K37_B	ΔASAAver
Val45	25.0	18.8	33.7	24.6	18.5	24.1
Val53	27.8	29.1	21.9	26.9	30.3	27.2
Ile66	18.5	27.3	29.2	25.5	25.4	25.2
Met163	14.0	29.2	30.6	32.0	27.9	26.7
Ile174	27.4	41.5	26.8	32.7	34.6	32.6
Asp175	18.4	20.1	10.1	8.6	15.5	14.6

ΔASAAver: ΔASA averaged for the four inhibitors (for K37 two conformations are considered). See also Figure 5.

In general, as also exemplified in Table 3 by TBB and K25, each inhibitor responds in a different manner to the individual mutation of either V66 or I174, and the double mutation tends to display an additive or less than additive effect, reflecting subtle differences in binding and suggesting that the inhibitor adopts a different conformation in the mutated site in order to partially compensate the lost interactions with new ones (note in this respect that in the case of TBB the double mutation is less effective than that of V66 alone). In this context, K44 represents a remarkable exception in that (1) it is equally susceptible to either the V66 or the I174 mutations, and (2) the efficacy of the double mutation is much more than additive, giving rise to a CK2 form which is practically insensitive to the inhibitor. In this respect the combined usage of K44 and the CK2 double mutant V66A, I174A appears as the first choice strategy to probe the real implication of CK2 in a cellular function whenever one wants to disprove the suspect that the inhibitor operates through alternative targets, other than CK2.

Significance

The main lesson to be drawn from the data presented is that closely related compounds sharing an identical scaffold can bind to the active site of the same protein kinase in substantially different manners as a consequence of subtle structural alterations. In the case considered (protein kinase CK2 and TBB related inhibitors), the 10-fold range variation in K_i (40–400 nM) cannot be correlated in a straightforward manner to the number and type of polar interactions observed; these interactions do, however, play an important role in the orientation of each individual ligand inside the binding pocket. For this class of ligands, the extent of the hydrophobic interactions (mediated by the common tetrabromo-benzimidazole scaffold) is ultimately responsible for their rank in potency. Two important corollaries are, first, that the features of this class of ligands are different from what is generally observed with other kinase inhibitors (whose binding potency is often increased mainly because of an improvement in the number or quality of polar interactions, notably hydrogen bonds) and, second, that subtle differences such as those outlined here are hardly predictable by modeling, which makes the experimental approach the only reliable tool for their elucidation. The structural information provided here can be applied to

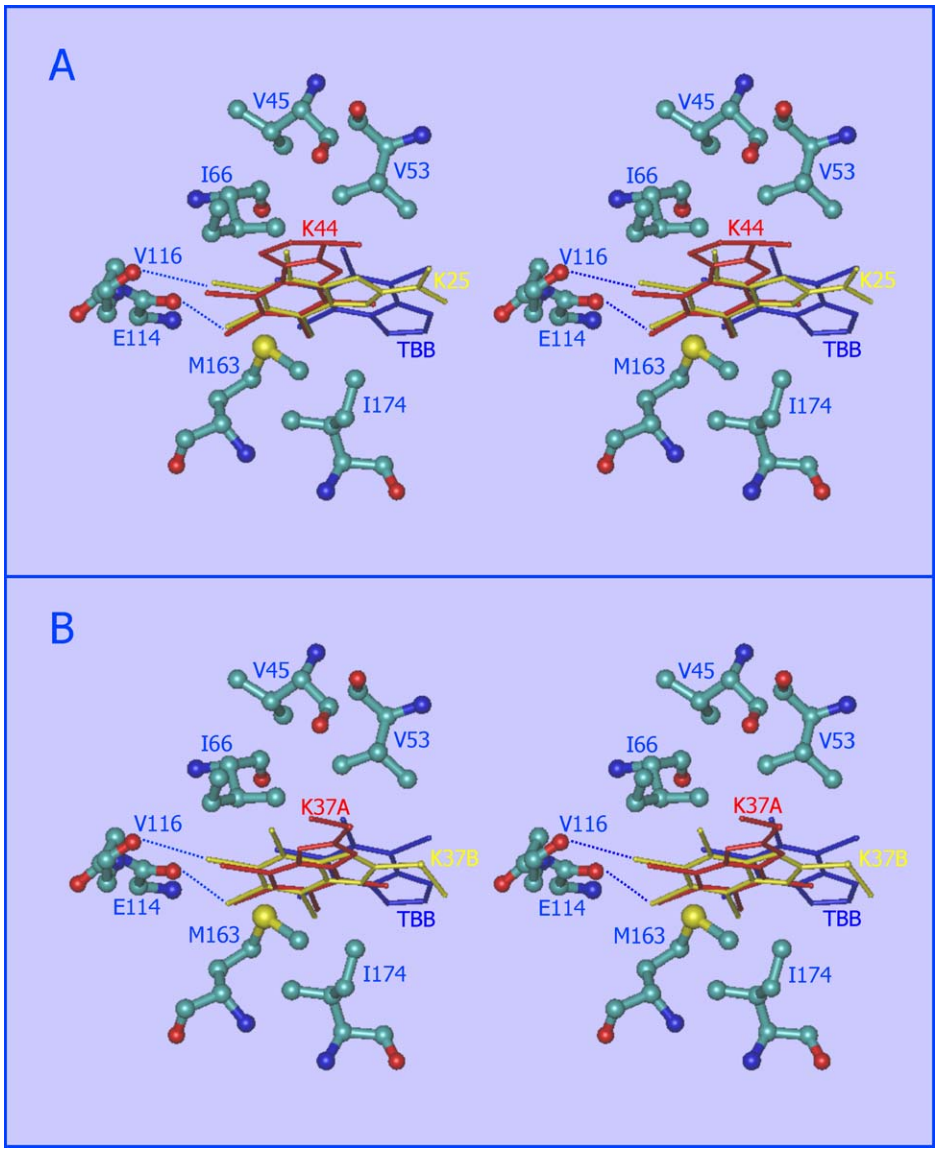

Figure 5. Stereo Representation of the Main Hydrophobic Residues Surrounding the Inhibitors in the ATP Binding Pocket

(A) K44 (red), K25 (yellow), and TBB (blue). (B) K37 in the two conformations A (red) and B (yellow) and TBB (blue). Halogen bonds with two residues (Glu114 and Val116) of the hinge region are indicated by blue dotted lines. (See also Table 2.)

further improve the inhibitory potency of TBB derivatives, without losing selectivity.

Experimental Procedures

Synthesis of K44 (N^1,N^2-Ethylene-2-Methylamino-4,5,6,7-Tetrabromo-Benzimidazole)

All chemicals and solvents were purchased from Sigma-Aldrich. Melting points were measured in open capillary tubes on a Gallenkamp-5 melting point apparatus. ^{1}H NMR spectra (in ppm) were measured with Varian Gemini 200 MHz and Varian UNITYplus spectrometers at 298 K in dimethyl sulfoxide (DMSO)-d_6 using tetramethylsilane as internal standard.

Mass spectra (70 eV) were obtained with ADM-604 (Intectra) spectrometer. Elemental analyses (C, H, N) of new compounds were within ±0.4% of the respective theoretical values.

2-(2-Hydroxyethyl)Methylamino)-4,5,6,7-Tetrabromobenzimidazole (2)

The mixture of **1** (4 g, 7.8 mmol) and 2-(methylamino)ethanol (8 ml, 100 mmol) in n-propanol (35 ml) was stirred and refluxed for 24 hr. Next, water (20 ml) was added and the solution was brought to pH 5 with acetic acid. The formed precipitate was filtered, washed thoroughly with water and dried in vacuum (2.35 g, 59%). The chromatographic pure compound was used for the further step without crystallization. The sample for analytical and enzymatic investigations was crystallized from ethanol. M.p. 243-245ºC. ^{1}H NMR: 3.18 (s, CH_3), 3.64 (t, CH_2) 4.95 (bs, OH), 11.4 (bs, NH-benzim.); MS: 509 (23), 507 (35), 505 (24), 478 (24), 476 (36), 474 (25), 467 (16), 465 (64), 463 (100), 461 (69), 459 (18).

N^1,N^2-Ethylene-2-Methylamino-4,5,6,7-Tetrabromobenzimidazole (3) (4,5,6,7-tetrabromo-1-methyl-2,3-dihydro-1H-1,3a,8-triaza-cyclopenta[a]indene)

The suspension of **2** (1.2 g, 2.35 mmol) in thionyl chloride (12 ml) was stirred and refluxed for 1 hr. The pale yellow solution was evaporated to dryness and then twice with ethanol (2× 50 ml). To the residue EtOH (45 ml) and DBU (1.5 ml, 10 mmol) was added and stirred and refluxed for 2 hr. The reaction mixture was treated with water (20 ml) and left to crystallize. The white, chromatographically pure precipitate formed (0.81 g, 70%) was filtered and washed with water. For analytical purposes the sample was crystallized from ethanol.

Table 3. IC_{50} Values of TBB and TBB Derivatives Relative to CK2, Val66Ala, and/or Ile174Ala Mutants and CDK2/Cyclin A

Inhibitor	IC_{50} values (μM)					Ratio IC_{50} (CDK2/CK2)
	CK2	V66A	I174A	V66A,I174A	CDK2	
TBB	0.50[a]	13.0	1.74	12.5	15.6[b]	31.2
K44	0.74	34.1	34.4	168	6.90[c]	9.3
K37	0.25	—	—	—	1.17	4.7
K25	0.14	1.78	3.30	5.79	3.12	22.3

[a] Data from [24].
[b] Data from [30].
[c] This value may represent an underestimate because, although 50% inhibition is obtained at about 7 μM K44, by increasing the inhibitor concentration up to 25 μM inhibition remains at about the same level.

M.p. > 300ºC. ^{1}H NMR: 2.97 (s, CH_3), 3.95 (t, CH_2), 4.39 (t, CH_2); MS: 492 (16), 490 (64), 488 (100), 486 (69), 484 (18).

CK2 and CK2 Mutants

For kinetic experiments human CK2α wild-type and mutants V66A and V66A,I174A were expressed and purified as described previously [48]. CK2α mutants and IC_{50} values were obtained as previously reported [36].

CDK2/CyclinA Phosphorylation Assays

Human CDK2/cyclinA [45] was kindly provided by Prof. Jane Endicott. Phosphorylation assays were carried out in the presence of increasing amounts of each inhibitor tested in a final volume of 30 μl containing 16 μl of buffer C (60 mM β-glycerophosphate, 25 mM MOPS, 5 mM EGTA, 15 mM $MgCl_2$, 30 mM 4-nitrophenyl phosphate, 1 mM dithiothreitol [DTT], 40 nM of affinity purified CDK2/cyclinA, 0.83 mg/ml of histone H1 (Sigma type III-S) and 0.0125 mM [33P-ATP] (500-1000 cpm/pmol). After 10 min incubation at 30ºC the reaction was stopped, spotting 25 μl onto Whatman P81 phosphocellulose. The filter were washed three times in 0.5% phosphoric acid and dried before counting.

Crystal Preparation and Data Collection

The recombinant CK2 α-subunit from *Zea mays* was expressed in *Escherichia coli*, isolated and purified according to a previously described method [37]. Crystals of the CK2 complexes with the three inhibitors K44 (N^1,N^2-ethylene-2-methylamino-4,5,6,7-tetrabromobenzimidazole), K25 (4,5,6,7-tetrabromo-2-(dimethylamino) benzimidazole), and K37 (S-methyl-4,5,6,7-tetrabromo-benzimidazole) were obtained by cocrystallization with the sitting drop vapor-diffusion technique. The 8 mg/ml protein stock solution was preincubated with a 100 mM inhibitor solution (100% DMSO) in the proper amount to have an inhibitor-protein molar ratio of 3:1, and not to exceed a 5% DMSO concentration in the final protein solution.

Crystallization trails were performed by mixing a 2 μl drop of preincubated stock solution with 4 μl of water and 2 μl of precipitant solution (10%–20% PEG 4000, sodium acetate 0.2 M, Tris 0.1 M pH 8). The drop was equilibrated against 500 μl of the same precipitant solution (20% PEG 4000). Crystals grew in few days at 293 K.

For all the three inhibitors X-ray diffraction data were collected at the X-ray diffraction beam-line of the ELETTRA synchrotron facility on a Mar CCD detector, at a temperature of 100 K. Before mounting, crystals were cryoprotected by a very rapid soaking in type B immersion oil (Hampton Research). Statistics on data collection are reported in Supplemental Table S1. Data were indexed with MOSFLM [49] and then scaled with SCALA from the CCP4 software package [50].

Structure Determination and Refinement

All three enzyme-inhibitor complexes crystallize in the space group C2, with one molecule in the asymmetric unit. All maize CK2α crystal structures known so far belong to this space group, with the exception of the complex with TBB that crystallized in the space group P1 [37]. As discussed in ref [43], the "stretched" **b** cell parameters and the β angles (Table S1) are compatible with the extended conformations of the loop 102–108, and indeed this is what is found in the final models. The fact that now a silicon oil was used as cryoprotectant seems to confirm that the shrinkage in the unit cell dimensions observed in previous crystal data was due to the use of high concentration of dehydrating substances as PEG or glycerol as cryoprotectants.

To find the best position inside the unit cell, an initial rigid body transformation on the model of the apoenzyme was adequate, using the CNS software package [51]. The refinement was carried out using SHELX [52] for K25 and K44 and CNS for K37, for which data at only 2.3 Å resolution were available. The presence of the inhibitor in the active site was clear since the beginning of the refinement in both |Fo − Fc| and |2Fo − Fc| maps for all three compounds. The presence of high peaks of electron density corresponding to the bromine atoms made the positioning of the inhibitors straightforward (see Supplemental Figure S1, available with this article online). The initial extended electron density for K37 suggested a double orientation for this inhibitor in the active site, as confirmed by the subsequent refinement.

The definition files for the inhibitors were initially created by HicUp [53], corrected with the adequate parameters and used in the whole refinement procedures that was carried out alternating automated cycles and manual inspection steps using the graphic program QUANTA [54]. During the final steps of the refinement, water molecules, chloride ions (one in K25 and one in K44 complex), and a DMSO molecule (in K25 complex) were added. The assignment of peaks in the electron density to chloride ions have been made on the basis of the intensity of the peaks (more than five sigma) and the geometry and nature of the coordination ligands around the peaks (water molecules and nitrogen atoms, at distances between 3.1 and 3.4 Å; see Figure 2 for details). A check in the Macromolecular Structure Database (www.ebi.ac.uk/msd/index.html) confirmed that the chlorine ion coordination in our models is in agreement with the examples reported in the database.

The stereochemistry and geometric properties of the models were checked with the program PROCHECK [55] and proved to be completely adequate for the respective resolutions, with no residues in disallowed regions of the Ramachandran plot. Statistics on final models are reported in Supplemental Table S1.

Structural Analysis

Calculation of the Accessible Surface Areas (ASA) and their differences (ΔASA) have been performed with the program Areaimol from the CCP4 suite, with a probe of 1.4 Å radius and a parameter PTNDEN = 100 for the best accuracy. The program Contact from the CCP4 suite has been utilized for the calculation of atom distances, with two cutoffs of 3.7 and 3.9 Å, as reported in Table 2.

Supplemental Data

A Supplemental Scheme, Supplemental Table, and Supplemental Figure are available online at http://www.chembiol.com/cgi/content/full/12/11/1211/DC1/.

Acknowledgments

We are grateful to staff at the ELETTRA synchrotron, Trieste, Italy, for help during diffraction measurements and to Professor Jane Endicott for kindly providing protein kinase CDK2. This work was supported by Ministero Italiano della Salute (Italian Ministry of Health), by Associazione Italiana per la Ricerca sul Cancro (AIRC; Italian Association for Cancer Research) and by grants from the Ministero dell'Istruzione, dell'Università e della Ricerca (MIUR; Ministry of Education and Research) (PRIN 2003 to L.A.P. and PRIN 2004 to R.B.) and from the European Union (Integrated EU Project "Prokinase research" LSHB-CT-2004-503467).

Received: May 13, 2005
Revised: August 2, 2005
Accepted: August 12, 2005
Published: November 18, 2005

References

1. Manning, G., Whyte, D.B., Martinez, R., Hunter, T., and Sudarsanam, S. (2002). The protein kinase complement of the human genome. Science *298*, 1912–1934.

2. Blume-Jensen, P., and Hunter, T. (2001). Oncogenic kinase signalling. Nature *411*, 355–365.
3. Cohen, P. (2002). Protein kinases–the major drug targets of the twenty-first century? Nat. Rev. Drug Discov. *1*, 309–315.
4. Sawyers, C.L. (2002). Rational therapeutic intervention in cancer: kinases as drug targets. Curr. Opin. Genet. Dev. *12*, 111–115.
5. Fabbro, D., Parkinson, D., and Matter, A. (2002). Protein tyrosine kinase inhibitors: new treatment modalities? Curr. Opin. Pharmacol. *2*, 374–381.
6. Pinna, L.A. and Cohen, P.T.W., eds. (2005). Inhibitors of Protein Kinases and Protein Phosphatases. Handbook of Experimental Pharmacology 167 (Berlin Heidelberg: Springer-Verlag).
7. Noble, M.E., Endicott, J.A., and Johnson, L.N. (2004). Protein kinase inhibitors: insights into drug design from structure. Science *303*, 1800–1805.
8. Traxler, P., and Furet, P. (1999). Strategies toward the design of novel and selective protein tyrosine kinase inhibitors. Pharmacol. Ther. *82*, 195–206.
9. Schindler, T., Bornmann, W., Pellicena, P., Miller, W.T., Clarkson, B., and Kuriyan, J. (2000). Structural mechanism for STI-571 inhibition of Abelson tyrosine kinase. Science *289*, 1938–1942.
10. Gassel, M., Breitenlechner, C., Herrero, S., Engh, R., and Bossemeyer, D. (2005). Inhibitors of PKA and Related Protein Kinases. In Inhibitors of protein kinases and protein phosphatases. Handbook of Experimental Pharmacology 167. L.A. Pinna and P.T.W. Cohen, eds. (Berlin Heidelberg: Springer-Verlag), pp. 85–124.
11. Battistutta, R., Sarno, S., and Zanotti, G. (2005). Inhibitors of Protein Kinase CK2: Structural Aspects. In Inhibitors of protein kinases and protein phosphatases. Handbook of Experimental Pharmacology 167. L.A. Pinna and P.T.W. Cohen, eds. (Berlin Heidelberg: Springer-Verlag), pp. 125–155.
12. Meggio, F., and Pinna, L.A. (2003). One-thousand-and-one substrates of protein kinase CK2? FASEB J. *17*, 349–368.
13. Pinna, L.A. (2003). The raison d'etre of constitutively active protein kinases: the lesson of CK2. Acc. Chem. Res. *36*, 378–384.
14. Pinna, L.A. (2002). Protein kinase CK2: a challenge to canons. J. Cell Sci. *115*, 3873–3878.
15. Litchfield, D.W. (2003). Protein kinase CK2: structure, regulation and role in cellular decisions of life and death. Biochem. J. *369*, 1–15.
16. Niefind, K., Guerra, B., Ermakowa, I., and Issinger, O.G. (2001). Crystal structure of human protein kinase CK2: insights into basic properties of the CK2 holoenzyme. EMBO J. *20*, 5320–5331.
17. Tawfic, S., Yu, S., Wang, H., Faust, R., Davis, A., and Ahmed, K. (2001). Protein kinase CK2 signal in neoplasia. Histol. Histopathol. *16*, 573–582.
18. Seldin, D.C., and Leder, P. (1995). Casein kinase II alpha transgene-induced murine lymphoma: relation to theileriosis in cattle. Science *267*, 894–897.
19. Kelliher, M.A., Seldin, D.C., and Leder, P. (1996). Tal-1 induces T cell acute lymphoblastic leukemia accelerated by casein kinase IIalpha. EMBO J. *15*, 5160–5166.
20. Orlandini, M., Semplici, F., Ferruzzi, R., Meggio, F., Pinna, L.A., and Oliviero, S. (1998). Protein kinase CK2alpha' is induced by serum as a delayed early gene and cooperates with Ha-ras in fibroblast transformation. J. Biol. Chem. *273*, 21291–21297.
21. Landesman-Bollag, E., Channavajhala, P.L., Cardiff, R.D., and Seldin, D.C. (1998). p53 deficiency and misexpression of protein kinase CK2alpha collaborate in the development of thymic lymphomas in mice. Oncogene *16*, 2965–2974.
22. Wang, G., Ahmad, K.A., and Ahmed, K. (2005). Modulation of death receptor-mediated apoptosis by CK2. Mol. Cell. Biochem. *274*, 201–205.
23. Critchfield, J.W., Coligan, J.E., Folks, T.M., and Butera, S.T. (1997). Casein kinase II is a selective target of HIV-1 transcriptional inhibitors. Proc. Natl. Acad. Sci. USA *94*, 6110–6115.
24. Sarno, S., de Moliner, E., Ruzzene, M., Pagano, M.A., Battistutta, R., Bain, J., Fabbro, D., Schoepfer, J., Elliott, M., Furet, P., et al. (2003). Biochemical and three-dimensional-structural study of the specific inhibition of protein kinase CK2 by [5-oxo-5,6-dihydroindolo-(1,2-a)quinazolin-7-yl]acetic acid (IQA). Biochem. J. *374*, 639–646.
25. Yim, H., Lee, Y.H., Lee, C.H., and Lee, S.K. (1999). Emodin, an anthraquinone derivative isolated from the rhizomes of *Rheum palmatum*, selectively inhibits the activity of casein kinase II as a competitive inhibitor. Planta Med. *65*, 9–13.
26. Meggio, F., Pagano, M.A., Moro, S., Zagotto, G., Ruzzene, M., Sarno, S., Cozza, G., Bain, J., Elliott, M., Deana, A.D., et al. (2004). Inhibition of protein kinase CK2 by condensed polyphenolic derivatives: an in vitro and in vivo study. Biochemistry *43*, 12931–12936.
27. Vangrevelinghe, E., Zimmermann, K., Schoepfer, J., Portmann, R., Fabbro, D., and Furet, P. (2003). Discovery of a potent and selective protein kinase CK2 inhibitor by high-throughput docking. J. Med. Chem. *46*, 2656–2662.
28. Kazimierczuk, Z., Stolarski, R., and Shugar, D. (1985). Stereospecific synthesis by the sodium salt glycosylation method of halogeno benzimidazole 2′-deoxyribose analogues of the inhibitor of hnRNA synthesis, 5,6-dichloro-1-(beta-D-ribofuranosyl)-benzimidazole (DRB). Z. Naturforsch. [C] *40*, 715–720.
29. Zandomeni, R., Zandomeni, M.C., Shugar, D., and Weinmann, R. (1986). Casein kinase type II is involved in the inhibition by 5,6-dichloro-1-beta-D-ribofuranosylbenzimidazole of specific RNA polymerase II transcription. J. Biol. Chem. *261*, 3414–3419.
30. Sarno, S., Reddy, H., Meggio, F., Ruzzene, M., Davies, S.P., Donella Deana, A., Shugar, D., and Pinna, L.A. (2001). Selectivity of 4,5,6,7-tetrabromobenzotriazole, an ATP site-directed inhibitor of protein kinase CK2 ('casein kinase-2'). FEBS Lett. *496*, 44–48.
31. Ruzzene, M., Penzo, D., and Pinna, L.A. (2002). Protein kinase CK2 inhibitor 4,5,6,7-tetrabromobenzotriazole (TBB) induces apoptosis and caspase-dependent degradation of haematopoietic lineage cell-specific protein 1 (HS1) in Jurkat cells. Biochem. J. *364*, 41–47.
32. Loizou, J.I., El-Khamisy, S.F., Zlatanou, A., Moore, D.J., Chan, D.W., Qin, J., Sarno, S., Meggio, F., Pinna, L.A., and Caldecott, K.W. (2004). The protein kinase CK2 facilitates repair of chromosomal DNA single-strand breaks. Cell *117*, 17–28.
33. Miyata, Y., and Nishida, E. (2004). CK2 controls multiple protein kinases by phosphorylating a kinase-targeting molecular chaperone, Cdc37. Mol. Cell. Biol. *24*, 4065–4074.
34. Di Maira, G., Salvi, M., Arrigoni, G., Marin, O., Sarno, S., Brustolon, F., Pinna, L.A., and Ruzzene, M. (2005). Protein kinase CK2 phosphorylates and upregulates Akt/PKB. Cell Death Differ. *12*, 668–677.
35. Sarno, S., Ruzzene, M., Frascella, P., Pagano, M.A., Meggio, F., Zambon, A., Mazzorana, M., Di Maira, G., Lucchini, V., and Pinna, L.A. (2005). Development and exploitation of CK2 inhibitors. Mol. Cell. Biochem. *274*, 69–76.
36. Pagano, M.A., Andrzejewska, M., Ruzzene, M., Sarno, S., Cesaro, L., Bain, J., Elliott, M., Meggio, F., Kazimierczuk, Z., and Pinna, L.A. (2004). Optimization of protein kinase CK2 inhibitors derived from 4,5,6,7-tetrabromobenzimidazole. J. Med. Chem. *47*, 6239–6247.
37. Battistutta, R., De Moliner, E., Sarno, S., Zanotti, G., and Pinna, L.A. (2001). Structural features underlying selective inhibition of protein kinase CK2 by ATP site-directed tetrabromo-2-benzotriazole. Protein Sci. *10*, 2200–2206.
38. Toledo, L.M., Lydon, N.B., and Elbaum, D. (1999). The structure-based design of ATP-site directed protein kinase inhibitors. Curr. Med. Chem. *6*, 775–805.
39. Scapin, G. (2002). Structural biology in drug design: selective protein kinase inhibitors. Drug Discov. Today *7*, 601–611.
40. Pagano, M.A., Meggio, F., Ruzzene, M., Andrzejewska, M., Kazimierczuk, Z., and Pinna, L.A. (2004). 2-Dimethylamino-4,5,6,7-tetrabromo-1H-benzimidazole: a novel powerful and selective inhibitor of protein kinase CK2. Biochem. Biophys. Res. Commun. *321*, 1040–1044.
41. Andrzejewska, M., Pagano, M.A., Meggio, F., Brunati, A.M., and Kazimierczuk, Z. (2003). Polyhalogenobenzimidazoles: synthesis and their inhibitory activity against casein kinases. Bioorg. Med. Chem. *11*, 3997–4002.
42. Battistutta, R., Sarno, S., De Moliner, E., Papinutto, E., Zanotti, G., and Pinna, L.A. (2000). The replacement of ATP by the competitive inhibitor emodin induces conformational modifications in the catalytic site of protein kinase CK2. J. Biol. Chem. *275*, 29618–29622.

43. De Moliner, E., Moro, S., Sarno, S., Zagotto, G., Zanotti, G., Pinna, L.A., and Battistutta, R. (2003). Inhibition of protein kinase CK2 by anthraquinone-related compounds: a structural insight. J. Biol. Chem. *278*, 1831–1836.
44. Niefind, K., Putter, M., Guerra, B., Issinger, O.G., and Schomburg, D. (1999). GTP plus water mimic ATP in the active site of protein kinase CK2. Nat. Struct. Biol. *6*, 1100–1103.
45. De Moliner, E., Brown, N.R., and Johnson, L.N. (2003). Alternative binding modes of an inhibitor to two different kinases. Eur. J. Biochem. *270*, 3174–3181.
46. Lommerse, J.P.M., Stone, A.J., Taylor, R., and Allen, F.H. (1996). The nature and geometry of intermolecular interactions between halogens and oxygen or nitrogen. J. Am. Chem. Soc. *118*, 3108–3116.
47. Auffinger, P., Hays, F.A., Westhof, E., and Ho, P.S. (2004). Halogen bonds in biological molecules. Proc. Natl. Acad. Sci. USA *101*, 16789–16794.
48. Sarno, S., Vaglio, P., Meggio, F., Issinger, O.G., and Pinna, L.A. (1996). Protein kinase CK2 mutants defective in substrate recognition: purification and kinetic analysis. J. Biol. Chem. *271*, 10595–10601.
49. Leslie, A.G.W. (1991). Molecular data processing. In Crystallographic Computing V. D. Moras, A.D. Podjarny and J.P. Thierry, eds. (Oxford: Oxford University Press), pp. 50–61.
50. CCP4 (1994). The CCP4 suite: programs for protein crystallography. Acta Crystallogr. *D50*, 760–763.
51. Brunger, A.T., Adams, P.D., Clore, G.M., DeLano, W.L., Gros, P., Grosse Kunstleve, R.W., Jiang, J.S., Kuszewski, J., Nilges, M., Pannu, N.S., et al. (1998). Crystallography & NMR system: a new software suite for macromolecular structure determination. Acta Crystallogr. D Biol. Crystallogr. *54*, 905–921.
52. Sheldrick, G.M., and Schneider, T.R. (1997). SHELXL: high-resolution refinement. Methods Enzymol. *277*, 319–343.
53. Kleywegt, G.J., and Jones, T.A. (1998). Databases in protein crystallography. Acta Crystallogr. D *54*, 1119–1131.
54. Accelrys (1998). QUANTA Version 98.1111 (computer program). Accelrys, San Diego, California.
55. Laskowski, R.A., MacArthur, M.W., Moss, D.S., and Thornton, J.M. (1993). PROCHECK: a program to check the stereochemical quality of protein structure. J. Appl. Crystallogr. *26*, 283–291.

Accession Numbers

The coordinates for the models of the K25, K44, and K37 complexes have been deposited at the RCSB Protein Data Bank with IDs 1ZOE, 1ZOH, and 1ZOG, respectively.